Photodissociation dynamics of NH_2OH from the first absorption band

K.-H. Gericke, M. Lock, F. Schmidt, and F. J. Comes
Institut für Physikalische und Theoretische Chemie der Johann Wolfgang Goethe-Universität, Marie-Curie-Strasse 11, D-60439 Frankfurt am Main, Federal Republic of Germany

(Received 15 March 1994; accepted 12 April 1994)

The dynamics of the photofragmentation of hydroxylamine from its lowest excited electronic state, $\tilde{A}\ ^1A'$, have been investigated. The main dissociation channel leads to H+H+HNO with a quantum efficiency of 1.7 for hydrogen atoms. The H atoms have been analyzed by laser induced fluorescence using a frequency tripled dye laser with sub-Doppler resolution. A sequential decay process is proposed where the first ejected H fragment leaves a highly vibrationally excited intermediate which dissociates after intramolecular vibrational redistribution into H+HNO. Another photodissociation channel leads to $OH(X\ ^2\Pi)$ and $NH_2(\tilde{A}\ ^2A_1)$. $NH_2(\tilde{A})$ has been detected by its emission spectrum, $\tilde{A}\ ^2A_1 \rightarrow \tilde{X}\ ^2B_1$, indicating strong vibrational excitation of the ν_2 bending mode. The OH product shows no vibrational excitation, whereas rotational states up to $N=20$ have been observed. Observation of the product state distributions and of the $\langle \boldsymbol{\mu} \cdot \mathbf{v} \rangle$ and $\langle \mathbf{v} \cdot \mathbf{J} \rangle$ correlations yield a qualitative picture of the upper potential energy surface (PES). Out of the nine coordinates characterizing the normal vibrational modes of H_2NOH only the NO distance, the NOH bending angle (responsible for OH rotation), and the NH_2 bending angle (responsible for NH_2 bending motion) are involved in the NH_2+OH fragmentation channel.

I. INTRODUCTION

Hydroxylamine in its electronic ground state is a well-characterized stable molecule. The equilibrium geometry has been analyzed by microwave spectroscopy and the use of color center lasers.[1–3] *Ab initio* studies further clarified the geometry of the ground state.[4] NH_2OH is unique for being the simplest molecule with different numbers of lone pairs on adjacent atoms.[5] Photofragmentation in the electronic ground state has been studied by infrared-optical double resonance excitation of OH overtone levels.[6,7] Since the deposition of energy was sufficient to break the N–O bond, nascent OH fragments were detected by laser induced fluorescence (LIF). Due to the observed broad linewidth in the vibrational overtone spectra of a rotationally resolved transition in NH_2OH, a very fast dissociation process is expected.

Significantly less is known about the spectroscopy, photochemistry, and dissociation dynamics of electronic excited states of hydroxylamine. The first and to our knowledge only *ab initio* study related to low-lying electronic states has been performed by Staemmler.[8] Vertical excitation energies to the four lowest states were calculated at the CEPA level and transition dipole moments at the SCF level. The transitions to the two low-lying singlet states are allowed and rather strong. An electron occupying an orbital localized essentially on the nitrogen $(7a')$ or the oxygen $(2a'')$ atom is excited into an $(8a')$ orbital which is delocalized over N and O. This already implies a fragmentation of NH_2OH into NH_2 and OH. Indeed, a final product analysis in both the photolysis and the mercury-photosensitized decomposition of hydroxylamine suggests an initial decay into NH_2 and OH.[9,10] However, N_2O as a final product was also observed which may originate from secondary reaction of primary NH_2O or HNO fragments.[10,11]

In the present study nascent OH and NH_2 products in the photodissociation of hydroxylamine at 193.3 nm have been observed and their internal energy distributions, translational energies, and OH vector correlations have been analyzed in order to elucidate the fragmentation process. Additionally, the main dissociation channel leading to hydrogen atoms has been investigated. The quantum yield, translational energy and spatial distribution of the H atoms were detected by Doppler spectroscopy.

II. EXPERIMENT

NH_2OH has been photolyzed by an ArF excimer laser at 193 nm (Lambda Physik, EMG 102). Nascent H and OH fragments were analyzed by observing the laser-induced fluorescence with sub-Doppler resolution. $NH_2(\tilde{A}\ ^2A_1)$ was analyzed by spectral resolution of its $\tilde{A}\ ^2A_1 \rightarrow \tilde{X}\ ^2B_1$ resonance fluorescence light. Hydroxylamine was prepared according to the method of Hurd and Brownstein[12] and stored in a glass bulb at the temperature of liquid nitrogen after purification by repeated destillation in vacuum. All experiments were carried out in a fluorescence cell at room temperature through which hydroxylamine slowly flowed at a pressure of about 0.5 Pa controlled by a capacitance gauge. During the experiment NH_2OH was kept at 0 °C and a glass needle valve was regulated to adjust the inlet pressure. The observation cell was evacuated by an oil diffusion pump.

The $OH(X\ ^2\Pi)$ product was probed around 308 nm by an excimer laser pumped frequency doubled dye laser (Lambda Physik, FL 2002 E). The bandwidth of this laser system could be reduced to 0.1 cm^{-1} by an intracavity étalon which allowed to resolve the shape and the width of the $OH(A\ ^2\Sigma \leftarrow X\ ^2\Pi)$ rotational lines which contain information on vector correlations, translational energy, and internal energy of the partner product formed in the same dissociation process.[13,14] The LIF signal was monitored perpendicular to the photolyzing and analyzing laser beams with a photomultiplier tube equipped with f 1.0 imaging optics and an interference filter which allowed undispersed observation of the $A\ ^2\Sigma \rightarrow X\ ^2\Pi$ emission.

 0021-9606/94/101(3)/1988/8/$6.00

Formation of electronically excited species was investigated by observing the spectrally resolved fluorescence light by a 0.5 m Polychromator equipped with a grating of 3600 grooves/mm and an optical multichannel analyzer (POSMA, Spectroscopic Instruments). The resolution of this system was about $\Delta\lambda/\lambda \approx 10^{-4}$.

In order to detect hydrogen atoms, the $^2P \leftarrow {}^2S$ transition was excited by irradiating into the cell the frequency-tripled output of the dye laser around 365 nm. Third harmonic generation was realized by focusing the linearly polarized dye laser beam with a quartz lens ($f=10$ cm) into a 13 cm long cell containing 8 kPa of Kr. A LiF lens ($f=10$ cm) collimated the generated vacuum ultraviolet (VUV) radiation. The bandwidth at 121.6 nm was measured to be $\Delta\nu_l \simeq 1.25$ cm^{-1}. This was checked carefully by recording spectra of thermal D atoms at different high inert gas pressures (up to 1 kPa He) and long delay times (up to 1 ms). The obtained line profiles were deconvoluted with the Doppler width of thermal D atoms ($\Delta\nu_{T=300\ \mathrm{K}} = 0.72$ cm^{-1}) in order to obtain the bandwidth $\Delta\nu_l$ of the analyzing VUV laser beam. The pulse energy was in the range of 10^9–10^{10} photons at a calculated beam diameter of about 1 mm. The fluorescence signal of the excited H-atoms was observed by a solar blind multiplier (EMR 542G-08-18).

A series of baffles in the paths of all laser beams reduced the amount of scattered light. The delay time between the photolyzing and analyzing laser was 50 ns. For measurements of the vector correlations both laser beams were linearly polarized. The plane of polarization of the dye laser was rotated by $\lambda/2$ plates. The polarization of the photolysis laser beam was controlled by turning the polarizer. This laser beam arrangement allowed experiments at four different geometries (II,IV,V,VI) defined in a previous work.[13] The photomultiplier output was registered with a boxcar integrator (Stanford, SRS 250) and stored in a microcomputer after A/D conversion. The computer also controlled the tuning of the dye laser. All time events in the experiment were controlled by a four-channel trigger delay device (Stanford, DG 535).

III. RESULTS

The most striking observation at intense ArF excimer laser irradiation was the strong fluorescence light as result of the photodissociation of hydroxylamine which covered the whole spectral range from the VUV threshold to the near infrared (IR), the detection limit of our apparatus. The following species were identified from their characteristic spectral features: NO($A\ ^2\Sigma^+ \rightarrow X\ ^2\Pi$), OH($A\ ^2\Sigma \rightarrow X\ ^2\Pi$), NH($A\ ^3\Pi \rightarrow X\ ^3\Sigma$), and $NH_2(\tilde{A}\ ^2A_1 \rightarrow \tilde{X}\ ^2B_1)$. However, the fluorescence intensity for all species except NH_2 was strongly power dependent and decreased significantly faster than is expected for a one-photon process. Thus, multiphoton excitation processes are responsible for the formation of NO($A\ ^2\Sigma^+$), OH($A\ ^2\Sigma$), and NH($A\ ^3\Pi$). Results of these multiple photon experiments will be presented in a forthcoming paper.[15] In the following only results of the one-photon fragmentation of NH_2OH at 193.3 nm will be discussed. However, it should be mentioned that the light from spontaneous fluorescence could not completely be suppressed resulting in a relatively high noise level for the LIF signals of OH. We observed nascent OH($^2\Pi$), $NH_2(^2A_1)$, and H(^2S) products in the one-photon experiment, but no NH fragments, neither in the triplet ($^3\Sigma^-$,$^3\Pi$) nor in the singlet ($^1\Delta$,$^1\Pi$) states.

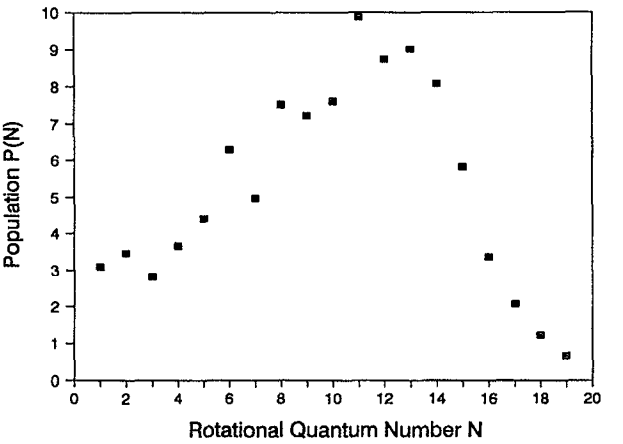

FIG. 1. Rotational state distribution $P(N)$ of nascent OH products formed in the photodissociation of NH_2OH at 193.3 nm. Plotted is $P(N)$ vs the rotational state N. Since no preferred formation of OH in a specific spin–orbit or in a Λ sublevel is observed $P(N)$ is the sum over the population of these fine-structure levels.

A. OH internal state distribution

The observed product state distribution of the OH fragment $P(q)$ generated in a quantum state q is determined from the integrated signal intensities $\int S(\nu)d\nu$, the transition probability B, and to a minor extent by the rotational alignment $\beta_{\mu J}$ which contains information on the vector correlation between the rotation of the product and the transition dipole moment $\boldsymbol{\mu}$ of the parent,

$$\int S(\nu)d\nu \sim P(q)\cdot B\cdot(b_0+b_1\beta_{\mu J}). \tag{1}$$

The geometry- and branch-dependent multipliers b_0 and b_1 have been calculated for observation of undispersed fluorescence.[13] The rotational state distribution of OH ($X\ ^2\Pi$, $v=0,N$) is shown in Fig. 1. Rotational states are populated up to $N=20$. In a "Boltzmann representation," the total distribution cannot be characterized by a straight line, i.e., no temperature parameter is associated to the rotational distribution. The average OH rotational energy is calculated to be $\langle E_{\mathrm{rot}}(\mathrm{OH})\rangle = \Sigma_N E_{\mathrm{rot}}(\mathrm{OH})\cdot P_N \simeq 2400$ cm^{-1}.

In the analysis of OH products, the R and P lines probe the symmetric $\Pi(A')$ state,[16] while the Q lines probe the $\Pi(A'')$ state which is slightly higher in energy.[17] An unequal population of the two Λ doublet states contains information on the planarity of the fragmentation process. No preferred population of a Λ doublet level was observed within the experimental error of 20%. Therefore, the rotational state distribution in Fig. 1 is given as the average of the $\Pi(A')$ and $\Pi(A'')$ state populations. The population of the two spin–orbit states, $\Pi_{3/2}$ and $\Pi_{1/2}$, of OH is also statistically distributed.

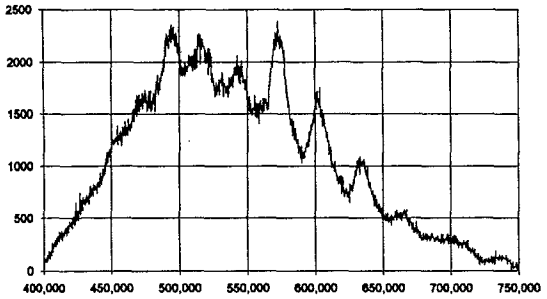

FIG. 2. $NH_2(\tilde{A}\ ^2A_1 \rightarrow \tilde{X}\ ^2B_1)$ fluorescence spectrum in the range from 400 to 750 nm observed after photodissociation of hydroxylamine at 193.3 nm. Units on the ordinate are arbitrary. The spectral features on the broad background can be attributed to the $\tilde{A}(\nu_1\nu_2\nu_3=050) \rightarrow \tilde{X}(0\nu_20)$ transitions.

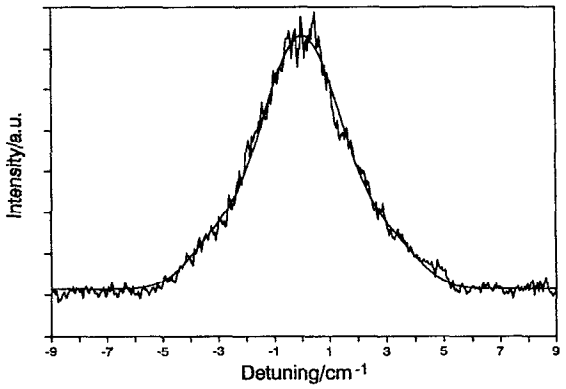

FIG. 3. Doppler profile of nascent hydrogen atoms generated in the photodissociation of NH_2OH at 193.3 nm. The solid line represents the fitted sum of two Doppler line functions. The quantum yield for the H atoms calculated from the integrated line intensity is $\phi_H \approx 1.7 \pm 0.2$.

The same spectral range that is employed for monitoring high rotational states of OH in $v=0$ also contains transitions from rotational states of vibrationally excited OH in $v=1$. No lines were observed which can be assigned to $OH(^2\Sigma\ v=1,\ J \leftarrow {}^2\Pi\ v=1, J)$ transitions when recording the 0–0 transition of OH. Therefore the OH product must essentially be formed in the lowest vibrational state $v=0$. An upper limit of $<5\%$ for the population in $v=1$ is obtained from the S/N ratio.

B. OH and NH_2 translational energies

The translational energy of a product can be extracted from the shape and the width of the absorption lines. From the Doppler shift, the OH recoil velocity and the kinetic energies of OH and NH_2 can be calculated—because of conservation of linear momentum. Details of the mathematical procedure are given in Ref. 18. We observed a mean OH recoil velocity of $v=(2600\pm200)$ m/s resulting in a mean translational energy of $\langle E_{\text{trans}}(\text{OH})\rangle = 4800\ \text{cm}^{-1}$. The mean kinetic energy of the NH_2 products is then given by

$$\langle E_{\text{trans}}(\text{NH}_2)\rangle = \frac{m_{\text{OH}}}{m_{\text{NH}_2}} \langle E_{\text{trans}}(\text{OH})\rangle \approx 5100\ \text{cm}^{-1}. \quad (2)$$

The mean translational energy of OH is higher than the mean rotational energy.

C. NH_2 internal energy distribution

The NH_2 fragment is the only product that is formed in an electronically excited state, $\tilde{A}\ ^2A_1$. The observed fluorescence spectrum is shown in Fig. 2. It covers the visible spectral range from 420 to 700 nm and can be assigned to the well-characterized $\tilde{A}\ ^2A_1 \rightarrow \tilde{X}\ ^2B_1$ electronic transition.[19] Since the electronic energy of the $\tilde{A}$ state is only $T_e = 10\,249\ \text{cm}^{-1}$, the spectral features must originate from highly vibrationally excited states of NH_2.

The work of Jungen *et al.*[20,21] is used to simulate spectra using their Franck–Condon factors and an arbitrarily chosen low rotational excitation. From the computations it is evident that the excited NH_2 fragments must have at least five vibrational quanta of $\nu_2=5$ in the ν_2 bending mode. The good agreement of the observed spectrum with the simulation assuming a low rotational excitation leads us to the conclusion that only low K-levels are populated in the NH_2 fragment.

We also performed measurements in order to observe NH_2 products generated in the electronic ground state. However, no laser-induced fluorescence was observed at the excitation wavelengths of the $\tilde{A} \leftarrow \tilde{X}$ transition. Due to strong background signals caused by the $NH_2(\tilde{A} \rightarrow \tilde{X})$ fluorescence light, the formation of nascent $NH_2(\tilde{X})$ cannot be completely excluded, but obviously significantly more electronically excited NH_2 is generated compared to NH_2 in the ground state.

D. Quantum yield and translational energy of the hydrogen atoms

We observed a strong signal when the frequency-tripled dye laser was tuned to the $^2P \leftarrow {}^2S$ transition of the H atom. Figure 3 shows a spectrum around this resonance transition. The detected signal $S(\nu)$ is given by

$$S(\nu) \sim (\phi_H I_p \sigma_p N) \cdot [I_{3\omega}(\nu)\sigma_H(\nu)], \quad (3)$$

where ϕ_H is the quantum efficiency for producing H atoms, I_p is the intensity of the photolysis laser, σ_p is the absorption cross section, and N is the concentration of parent molecules. $I_{3\omega}(\nu)$ is the intensity of the analyzing radiation around 121.6 nm and $\sigma_H(\nu)$ is the absorption cross section of the hydrogen atom at frequency ν. While the first bracket in Eq. (3) is proportional to the concentration of generated H atoms, the second bracket reveals the probability of observing these atoms.

Since the proportional constant in Eq. (3) is very difficult to determine, we decided to normalize the quantum yield $\phi_H(NH_2OH)$ to the quantum efficiency of hydrogen sulfide $[\phi_H(H_2S)=1]$; a procedure which was already successfully applied in the dissociation study of $HN_3 \rightarrow H+N_3$.[22] The LIF signal intensity of H atoms from the H_2S photodissociation is also given by Eq. (3) when the corresponding values of H_2S are used. Since the recoil velocity of the H atom depends on the parent molecule, the integrated signal intensity $\int S(\nu)d\nu$ was determined for H_2S and NH_2OH.

The observed LIF signal depends linearly on the intensity of the photolysis laser, hence two-photon processes can

be ruled out. Furthermore, the LIF signal is observed only when both lasers are working and only if the analyzing laser is fired after the photolyzing laser. The absorption cross sections for H_2S and NH_2OH at 193 nm are taken from the literature.[23] Applying Eq. (3) we calculated a quantum efficiency of $\phi_H = 1.7 \pm 0.2$ for the generation of hydrogen atoms in the photodissociation of hydroxylamine at 193.3 nm.

We fitted a Doppler profile to the observed line shown in Fig. 3 in order to obtain first information on the mean recoil velocity and translational energy. The Doppler shift was found to be $\Delta\nu_D \simeq 1.7$ cm^{-1} taking vector correlations into account and deconvoluting with the linewidth of the analyzing dye laser. This value corresponds to a mean H atom recoil velocity of $\langle v_H \rangle = c \cdot \Delta\nu_D/\nu_0 \simeq 6200$ m/s and a mean translational energy of $\langle E_{trans}(H) \rangle = 1650$ cm^{-1}. It should be emphasized that the quality of this fit is poor when only one Doppler profile function is used. However, the observed line shape is significantly better described by two profile functions (see solid line in Fig. 3). Details will be discussed in the next main chapter.

E. Vector correlations

The correlated vector properties of a fragmentation process provide a detailed understanding of the dynamics on the upper potential energy surface.[13,18,24] In the photodissociation of hydroxylamine the vectors of interest are the transition dipole moment $\boldsymbol{\mu}$ of NH_2OH, the recoil velocity $\mathbf{v}$, and the rotation $\mathbf{J}$ of the OH product.

This dynamical information can be extracted from the shape of the OH lines.[13] The important correlation between the translational and rotational motion of the OH fragment is easily obtained from observation of Q and P (or R) lines originating from the same rotational state. For a parallel alignment of $\mathbf{v}$ and $\mathbf{J}$ the P lines show a dip in the center of a Doppler profile in comparison to the corresponding Q lines. For a perpendicular alignment the behavior of the two branches is reversed. In this case Q lines exhibit a lower intensity in the center of the line, while the center intensity of P lines is increased. Qualitatively this behavior is independent of the observation geometry.[13]

The P-lines of all analyzed OH transitions in the photodissociation of NH_2OH exhibit a high intensity in the center and a much lower intensity in the wings whereas the Q lines show a rectangular profile or even a dip in the center of the line. Since P and Q line profiles are different in shape, the rotational and translational motion of the OH fragment are correlated to each other. The rotational vector $\mathbf{J}$ is aligned perpendicular to the recoil velocity $\mathbf{v}$ of the OH product and a negative $\langle \mathbf{v} \cdot \mathbf{J} \rangle$ correlation of OH characterizes the photofragmentation process of hydroxylamine at 193 nm.

The $\langle \boldsymbol{\mu} \cdot \mathbf{v} \rangle$ correlation is obtained by comparing OH lines measured at different detection geometries, i.e., when the alignment between the electromagnetic field vector $\mathbf{E}$ of the dissociating excimer laser beam and the observation direction $\mathbf{k}$ determined by the dye laser is varied.[13] When the propagation direction $\mathbf{k}$ of the analyzing laser beam is aligned perpendicular to the electric field vector $\mathbf{E}$ of the photolyzing laser beam, then for Q lines the intensity of the line center is lower than the intensity at the line wings. For a detection geometry with $\mathbf{k}$ and $\mathbf{E}$ being parallel to each other the profile is rectangular. This indicates a negative $\langle \boldsymbol{\mu} \cdot \mathbf{v} \rangle$ correlation and the transition dipole moment $\boldsymbol{\mu}$ ($\|\mathbf{E}$) of NH_2OH is aligned essentially perpendicular to the recoil velocity $\mathbf{v}$ of the OH product.

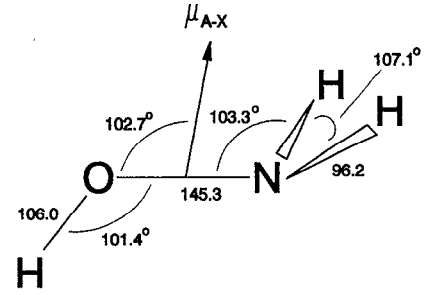

FIG. 4. Molecular structure of hydroxylamine in the electronic ground state. Units are pm for the bond distances and degrees for the angles.

A correlation between $\boldsymbol{\mu}$ and $\mathbf{J}$ influences mainly the intensity of a line [$\beta_{\mu J}$ in Eq. (1)], but only to a minor extent the profile of a line. Within the experimental error of 20% we observed no change in the intensities when OH LIF spectra were recorded at different geometries. Therefore, the alignment between the transition dipole of the parent molecule and the rotational vector of the OH product is of minor importance in the photodissociation of hydroxylamine at 193 nm. Similarily, an influence of the three vector correlation $\langle \boldsymbol{\mu} \cdot \mathbf{v} \cdot \mathbf{J} \rangle$ (Ref. 13) on the line profiles was not observed.

The other dissociation channel of hydroxylamine at 193 nm generating hydrogen products is also analyzed by the $\langle \boldsymbol{\mu} \cdot \mathbf{v} \rangle$ correlation which is measured by Doppler profiles. Since the observed recoil velocity of hydrogen atoms is very slow and the linewidth of the dye laser (1.25 cm^{-1}) is not much smaller than the Doppler shift (1.7 cm^{-1}), strong spectral features cannot be expected. A fit of a Doppler profile function to the measured line yields a value of $\beta_{\mu v} = 0.1 \pm 0.2$ for the anisotropy parameter.[13] Within the experimental error the H fragments are ejected isotropically in the photodissociation of NH_2OH at 193 nm.

IV. DISCUSSION

The molecular structure of hydroxylamine in the electronic ground state is shown in Fig. 4. The NH_2 group is in *trans*-position with respect to the OH group, at room temperature no *cis*-isomer is observed.[4] The OH bond (106 pm) is slightly longer than in the free radical (97 pm) and lies in the plane of C_S symmetry. It is strongly bent relative to the NO bond ($\alpha_{HOHN} \approx 101.4°$). The NH_2 plane and the NO bond enclose an angle of 67.3°.[5] The HNH group in hydroxylamine is also strongly bent ($\alpha_{HNH} \approx 107.1°$).

The electronic structure of NH_2OH in the ground state is given by the electronic configuration[8]

$$\tilde{X}\ ^1A' : 1a'^2 2a'^2 3a'^2 4a'^2 1a''^2 5a'^2 6a'^2 2a''^2 7a'^2.$$

Excitation of the $7a'$ orbital which is mainly localized on the N-atom to the $8a'$ orbital leads to the lowest electronic excited state of hydroxylamine, $\tilde{A}\ ^1A'$: $...2a''^2 7a' 8a'$. The

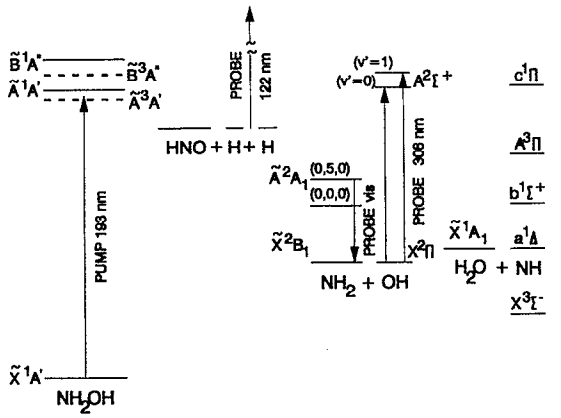

FIG. 5. Energetic level scheme in the photodissociation of hydroxylamine. NH products are not observed in one-photon processes.

second electronic excited state, $\tilde{B}\ ^1A''$: $...2a''7a'^2 8a'$ is reached by excitation of the $2a''$ orbital which is essentially a $2p$ lone pair-orbital localized on the O atom. The triplet states formed by the same electronic configurations will not significantly be excited because the transition probabilities are several orders of magnitude smaller than for the corresponding singlet–singlet transitions. Thus, only the singlet states $\tilde{A}\ ^1A'$ and $\tilde{B}\ ^1A''$ are important in the UV photodissociation of hydroxylamine. Staemmler calculated vertical excitation energies of 6.71 eV (185 nm) for the $\tilde{A} \leftarrow \tilde{X}$ transition and 7.36 eV (168 nm) for the $\tilde{B} \leftarrow \tilde{X}$ transition. Figure 5 shows an energy level scheme.

The measured UV absorption spectrum starts at about 225 nm and shows a first maximum at 182.5 nm.[11] Following a local minimum at 170 nm another strong absorption is observed. At wavelengths shorter than 160 nm no VUV absorption spectra are available. From the integrated line intensity of the first absorption band an oscillator strength of $f_{exp} \simeq 0.037$ is calculated. The *ab initio* calculation yields a value of $f_{theory} \simeq 0.038$. Due to the excellent agreement between theory and experiment with respect to both the position of the absorption maximum and the intensity, we expect that only the $\tilde{A}\ ^1A'$ state is excited when hydroxylamine is photolyzed at 193 nm. The transition dipole moment $\boldsymbol{\mu}$ for such a $A'-A'$ transition lies in the plane of symmetry which results in an angle of 77.3° between $\boldsymbol{\mu}$ and the NO axis in the direction of NH_2.[8]

The $8a'$ and $9a'$ orbitals are the linear combinations of the $3s$ atomic orbitals at O and N and at larger NO distances one of the two is expected to become the antibonding σ^* valence orbital, i.e., a fragmentation into NH_2 and OH takes place. For this process a dissociation energy of about 21 620 cm^{-1} is required.[6] In Table I the minimum energies and threshold wavelengths for the formation of different products are listed. The generation of NH fragments is energetically allowed. However, conservation of the electron spin restricts the possible electronic states of NH to the $a\ ^1\Delta$, $b\ ^1\Sigma^+$, and $c\ ^1\Pi$ singlet states. Since neither NH(X) nor OH(A) products in the one-photon dissociation of hydroxylamine at 193 nm are observed, the only partner product to the monitored ground state OH has to be NH_2 (cf. Table I), either in the

TABLE I. Possible products, required energies, and threshold wavelength λ_{thres} in the excitation of hydroxylamine. The applied UV photon energy in the present experiment is 51 730 cm^{-1}.

Products	Energy/cm^{-1}	λ_{thres}/nm	Comment
$NH_2OH(\tilde{A}\ ^1A')$	54 120	184.8	*ab initio* calculations[a]
$NH_2OH(\tilde{B}\ ^1A'')$	59 360	168.5	*ab initio* calculations[a]
$NH_2(\tilde{X})+OH(X)$	21 620	462.5	overtone dissociation[b]
$NH_2(\tilde{A})+OH(X)$	31 870	313.8	$NH_2(\tilde{X})+OH(X)+T_e(NH_2)$
$NH_2(\tilde{X})+OH(A)$	54 060	185.0	$NH_2(\tilde{X})+OH(X)+T_e(OH)$[c]
$H+NH(X\ ^3\Sigma^-)+OH$	52 630	190.0	thermodynamical data[d]
$H_2O+NH(X\ ^3\Sigma^-)$	11 360	880.3	thermodynamical data and
$+NH(a\ ^1\Delta)$	23 950	417.5	electronical energies[e]
$+NH(b\ ^1\Sigma^+)$	32 590	306.8	
$+NH(c\ ^1\Pi)$	54 710	182.8	
$+NH(A\ ^3\Pi)$	41 340	241.9	
NH_2+H+O	57 060	175.2	thermodynamical data
$H+HNO+H$	47 340	211.3	thermodynamical data
$H+H+NOH$	64 500	155.0	estimated[f]
H_2+NO+H	28 220	354.3	thermodynamical data
H_2+HNO	11 220	891.0	thermodynamical data

[a]Reference 8.
[b]Reference 6.
[c]Reference 25.
[d]Reference 26.
[e]Reference 27.
[f]Reference 28.

electronic ground state, $\tilde{X}\ ^2B_1$, or in the excited $\tilde{A}\ ^2A_1$ state (cf. Fig. 5). All other dissociation channels leading to OH or NH_2 can be excluded.

A. The OH+NH_2 channel

In order to discuss the origin of internal motion of the OH and NH_2 products, we will first consider the influence of initial parent motion on the observed product distributions. The influence of NH_2OH rotation on the fragment rotation can be estimated by simple classical calculations where parent rotation about the three axes of inertia is transferred into fragment internal rotation and orbital angular momentum. A simple break of the H_2N–OH bond is considered without any other influence from the upper PES. Assuming an energy content of $\frac{1}{2}kT = 104\ cm^{-1}$ for each degree of freedom, $J_\parallel = 1.4\hbar$ will be transferred into OH rotation where the rotational vector $\mathbf{J}$ is aligned along the recoil axis (positive $\langle \mathbf{v}\cdot\mathbf{J}\rangle$ correlation) and $J_\perp = 0.6\hbar$ for a perpendicular alignment between $\mathbf{v}$ and $\mathbf{J}$ (negative $\langle \mathbf{v}\cdot\mathbf{J}\rangle$ correlation). Since the OH fragments are generated with significantly more product rotation (up to $J_{OH} = 20.5\hbar$) and a negative $\langle \mathbf{v}\cdot\mathbf{J}\rangle$ correlation is found the observed fragment rotation and its alignment is not caused by initial parent rotation.

At room temperature most of the nine vibrational modes (Fig. 6) of hydroxylamine are not excited. Out of the symmetric vibrations (a') with respect to the symmetry plane of the molecule only the NH_2 wagging [$\nu_5(a') = 1117\ cm^{-1}$] and the NO stretch [$\nu_6(a') = 896\ cm^{-1}$] vibrational modes are populated to a small extent. The main vibrational energy of the parent is stored in the asymmetric H_2N–OH torsional mode [$\nu_9(a'') = 376\ cm^{-1}$]. However, the total vibrational energy of hydroxylamine at room temperature, $E_{vib}(H_2NOH, T = 300\ K) = 95\ cm^{-1}$ is negligibly small.

Still considering the influence of initial parent motion on the product state distributions, OH rotation can be induced only by zero point motions of the ν_4 NOH bending and ν_9

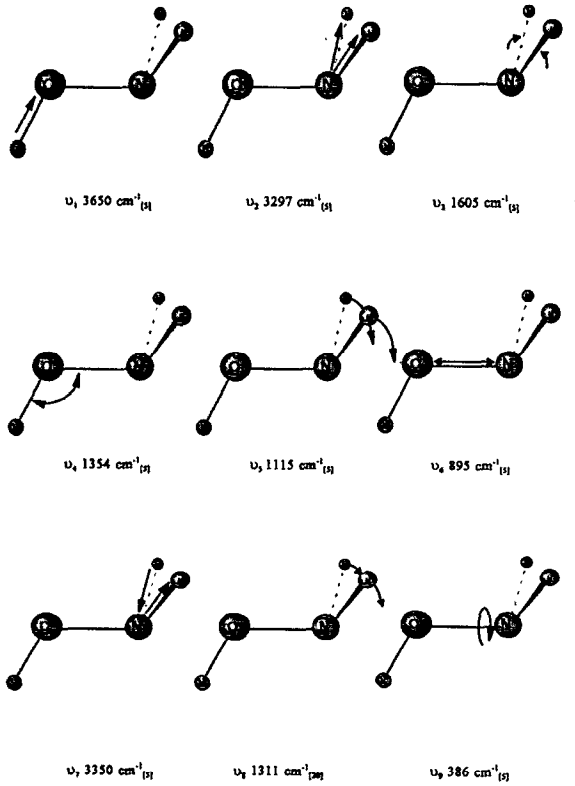

FIG. 6. Vibrational modes of NH_2OH. The first number is the experimentally observed vibrational energy (Refs. 1–4). The ν_8 NH_2 twisting mode has not been observed in the experiment, its energy value is calculated (Ref. 5).

torsion mode. Zero point motion of all other modes will essentially be released either as OH translation (ν_6) or vibration (ν_1) or will not at all influence the OH motion significantly. While the ν_9 torsional motion causes a parallel alignment between **v** and **J** of the OH product, the ν_4 HON bending motion results in a perpendicular alignment between the translational and rotational motion of the OH product. A simple calculation[29] shows that 47% ($\sim$320 cm^{-1}) of ν_4 and 44% ($\sim$120 cm^{-1}) of ν_9 zero point energy will be transferred into OH rotation. Since we observed a significantly higher rotational energy of OH and a negative $\langle \mathbf{v}\cdot\mathbf{J}\rangle$ correlation, the OH rotation is not determined by initial parent motion, neither rotation nor vibration, but by the dynamics on the upper potential energy surface (PES), i.e., by final state interaction.

For dynamical calculations Jacobian coordinates are appropriate to describe the photodissociation process because the separation coordinate R between the center of mass of OH and NH_2 is directly related to the linear momentum p, $dR/dt=p/\mu$. However, the upper PES can be described easier in a pictural way when normal coordinates, Fig. 6, are used.

The rotational excitation of OH and NH_2 is due to the torque provided by the gradient of the PES with respect to the bending angles between H_2–N–O (β) and between N–O–H (γ) and to the torsional angle δ (Fig. 5). The PES must be strongly dependent on the HON bending angle γ but not on the torsion angle δ due to the observed OH rotation. OH rotation induced via the torsional angle δ results in a positive $\langle \mathbf{v}\cdot\mathbf{J}\rangle$ correlation, while a bending angle dependence of the PES generates OH rotation with **J** perpendicular to **v**, i.e., with a negative $\langle \mathbf{v}\cdot\mathbf{J}\rangle$ correlation as observed in the experiment. If the dissociation proceeded via a torsional motion, the OH rotation would have to be compensated by NH_2 rotation in opposite direction, like in the photodissociation of H_2O_2.[30] In that case high N levels of NH_2 should be populated which is not confirmed by the experiment. However, generation of OH rotation via the HNO bending motion must not necessarily induce a significant amount of NH_2 rotation because the total angular momentum can always be conserved by the orbital angular momentum. Although we could not resolve the rotational excitation of NH_2 we expect low rotational excitation of this product, because the vibrational structure is well resolved. A very narrow NH_2 rotational distribution centered around a high rotation is unlikely because of the broad rotational distribution of the OH partner molecule.

Low populated K levels of NH_2 imply a low β dependence of the upper PES or a β dependence of the electronic excited PES which is similar to that of the ground state, $V_{ex}(\beta)\approx V_{gr}(\beta)+V_0$. A motion along the NH_2 twisting coordinate (ν_8 mode) should also be of minor importance. Since no vibrationally excited OH was observed, the dependence of the upper PES on the OH distance, r_{OH}, should also be comparable to that of the electronic ground state, $\partial V_{ex}(r_{OH})/\partial r_{OH}=0$.

The upper PES should strongly depend on the NH_2 bending angle α because the corresponding vibrational mode of the free radical is found to be significantly excited. A dependence of the upper PES on the N–H stretching coordinates (ν_2 and ν_7) cannot completely be ruled out but seems to be unlikely for the following reasons: we did not observe $NH_2(\tilde{A}\rightarrow\tilde{X})$ transitions which may be attributed to NH_2 stretching vibrations (small contributions of this vibration could overlap the peaks in Fig. 2). Thus, only NH_2 in the electronic ground state may be formed in excited NH stretching states, and we may have missed those molecules when the dye laser was tuned to the $\tilde{A}\rightarrow\tilde{X}$ electronic transition of NH_2. However, the observed OH Doppler width is another strong hint on the NH_2 product state population. Since the available energy E_{av} and internal energy of OH are well known, a measure of the translational energy of OH via the Doppler width directly reflects the internal energy of the OH partner fragment, i.e., the internal energy of NH_2.[30] An observed OH recoil velocity of 2600 m/s for the OH(N=9) state corresponds to an internal NH_2 energy of $E_{int}(NH_2)=E_{av}-E_{int}(OH)-E_{trans}(OH)-E_{trans}(NH_2)$ $=(30\,520-1\,650-4\,800-5\,100)\ cm^{-1}=18\,970\ cm^{-1}$ which is just a few hundred wave numbers above the ν_2=5, K=0 level of $NH_2(\tilde{A})$, the state from which the main NH_2 fluorescence originates. Thus, it is very likely that the partner fragments of OH are those NH_2 products which are identified by their resonance transitions, $\tilde{A}\ ^2A_1\rightarrow\tilde{X}\ ^2B_1$.

Upon a first view it may be surprising that NH_2 is formed in the $\tilde{A}\ ^2A_1$ state and not in highly vibrationally excited states of the ground state $\tilde{X}\ ^2B_1$. However, NH_2 is a textbook example of Renner–Teller coupling and the orbitals of the ground state and the excited state become equivalent

at 180°. Probably it is just a question of energy which state will be formed. If the assembled energy is higher than the electronic energy, $T_e=10\,250$ cm^{-1}, then NH_2 will be formed in the $\tilde{A}\,^2A_1$ state with the configuration $...(1b_2)^2(3a_1)(1b_1)^2$. Below T_e, NH_2 is formed in highly vibrationally excited bending states of $\tilde{X}\,^2B_1$ with the configuration $...(1b_2)^2(3a_1)^2(1b_1)$ but the bending vibrational motion is not sufficient to reach the degenerated linear configuration.

The dependence of the upper PES on the NO distance is obvious, because the fragments OH and NH_2 are formed. Repulsion along the NO axis which is close to a repulsion along the axis connecting the centers of mass of the two products will result in an essentially perpendicular alignment between the recoil direction **v** and the transition dipole moment $\boldsymbol{\mu}$ of the parent. This is confirmed by the negative $\langle\boldsymbol{\mu}\cdot\mathbf{v}\rangle$ correlation observed in the experiment.

In summary, from the nine normal coordinates (Fig. 6) only three seem to be essential to describe the dynamics of the 193 nm fragmentation of hydroxylamine into OH and NH_2; the NO separation coordinate, the HON bending angle γ (OH rotation), and the NH_2 bending angle α (NH_2 vibration). The released energy among the different degrees of freedom is summarized in Table II.

TABLE II. Observed mean energies in the photodissociation of H_2NOH at 193.3 nm. The available energy for the $NH_2(\tilde{X})+OH(X)$ channel is $E_a=30\,520$ cm^{-1}; $f_i=\langle E_i\rangle/E_a$.

	NH_2	OH
$\langle E_{el}\rangle$/cm^{-1}	10 250	0
$\langle E_{vib}\rangle$/cm^{-1}	7 300	0
$\langle E_{rot}\rangle$/cm^{-1}		2 400
$\langle E_{trans}\rangle$/cm^{-1}	5 100	4 800
f_{el}	0.34	0.0
f_{vib}	0.24	0.0
f_{rot}		0.08
f_{trans}	0.17	0.16

B. The hydrogen atom channel

One of the most surprising results in the photodissociation of hydroxylamine at 193 nm is the generation of hydrogen atoms with a quantum efficiency of greater than one. Thus, there should exist a dissociation channel in which more than one hydrogen atom is formed per absorbed photon. It was assured that the observed H atoms are indeed generated in a photodissociation process at 193 nm by variation of the delay time between photolysis and probe laser and by the (failed) attempt to monitor H atoms without radiation at 193 nm. The influence of impurities is negligibly small not only because of the purity of >99% but also because of the high absorption cross section of 3.4×10^{-18} cm^{-2} of NH_2OH at 193 nm. Any impurity must exhibit a differential cross section which has to be at least two orders of magnitude higher than the one of hydroxylamine.

Two photon processes can be ruled out because of the power dependence of the LIF-signal and the very low translational energy of the H products. If two absorbed photons at 193 nm would be responsible for the formation of H atoms than the available energy will be significantly higher, resulting most probably in fast recoiling hydrogen fragments.

There is only one product channel (see Table I) which is energetically accessible to generate two H atoms,

$$NH_2OH+h\nu(193\ \text{nm})\rightarrow H+HNO+H$$
$$\Delta E=47\,340\ \text{cm}^{-1}.$$

The average available energy for this process is $E_{av}=E_{h\nu}+E_{int}(NH_2OH)-\Delta E=52\,140\ \text{cm}^{-1}-47\,340\ \text{cm}^{-1}=4800$ cm^{-1} which has to be compared with the observed average translational energy for one H atom $\langle E_{trans}(H)\rangle=1650$ cm^{-1}.

One hydrogen fragment is generated by a break of the OH bond while the other H product results from a break of one of the two N–H bonds. In principle, a break of both N–H bonds would also lead to the formation of two H atoms. However, the formation of NOH as partner fragment needs much more energy than HNO. It should be mentioned that the enthalpy for NOH is not available in the literature, but from mean bond dissociation enthalpies a minimum energy of 64 500 cm^{-1} is calculated for the H+H+NOH channel (Table I). This value is well above the photon energy so that this dissociation channel can be excluded even if possible uncertainties using mean bond dissociation enthalpies are taken into account.

A simple MO picture cannot explain the formation of H atoms in the photolysis of NH_2OH because one would expect that the antibonding $4\sigma^*$ OH or $4a_1$ NH_2 states can only be excited at much higher energies. However, detailed *ab initio* calculation using double and triple ζ basis sets show that the excited states of NH_2OH are clearly antibonding with respect to NO but also with respect to OH and NH.[31] Thus, it is not surprising that NH_2OH can decay into H atoms and HNO.

A simultaneous ejection of two hydrogen products should result in similar recoil velocities for these two fragments. However, a stepwise decay, like

$$HONH_2\rightarrow H+ONH_2\rightarrow H+ONH+H$$

or

$$HONH_2\rightarrow HONH+H\rightarrow H+ONH+H$$

should generate H atoms with different velocities. In that case the observed H atom line profile should be composed of two Doppler profiles. Indeed, fitting the sum of two Doppler line functions to the measured H line significantly improved χ^2 and the residuals are distributed statistically. The obtained Doppler widths are $\Delta\nu_D(1)=(3.7\pm0.8)$ cm^{-1} and $\Delta\nu_D(2)=(1.3\pm0.3)$ cm^{-1} corresponding to recoil velocities ($v=c\cdot\Delta\nu_D/\nu_0$) of $v(1)=(13\,500\pm2\,900)$ ms^{-1} and $v(2)=(4\,700\pm1\,000)$ ms^{-1}. Translational energies calculated from these values are $E_{trans}(1)=(7\,700\pm3\,300)$ cm^{-1} and $E_{trans}(2)=(940\pm430)$ cm^{-1}. The relative contribution $f_D(1)$ and $f_D(2)$ of the individual Doppler lines to the total profile is also obtained by the fitting procedure $f_D(1)=0.58\pm0.06$ and $f_D(2)=0.42\pm0.05$. Thus, fast H atoms (1) are generated only with minor surplus compared to slow H atoms (2).

According to these results we assume the following fragmentation process: The two hydrogen atoms are generated in a sequential process. In a first step, the fast H(1) fragment is

ejected leaving a highly excited intermediate partner molecule (ONH_2 or HONH). The remaining energy in that intermediate is sufficient to break another H bond, but not the N–O bond. Thus, after intramolecular vibrational redistribution that molecule will finally dissociate into HNO and H(2). Since the remaining energy for HNO+H(2) is very low, these H(2) atoms can only be formed with very low recoil velocities. If the remaining energy stored in the intermediate is not sufficient to eject a H atom, then a highly excited molecule (H_2NO or HONH) should persist. However, since $f_D(1)$ is only slightly higher than $f_D(2)$, the main process in the photodissociation of hydroxylamine is the sequential ejection of two hydrogen atoms.

From the relative contribution $f_D(1)$ and $f_D(2)$ to the H atom Doppler profile we can calculate the maximum possible quantum efficiency ϕ_H^{max} in the absence of other fragmentation channels. In that case 81% of the dissociation process lead to one slow and one fast hydrogen atom and 19% lead to one fast H atom. Thus, ϕ_H^{max} is calculated to be $\phi_H^{max}=2\times0.81+0.19=1.81$. The experimentally observed quantum yield of $\phi_H^{exp}=1.7$ implies that the OH product of the other dissociation channel is formed with a quantum efficiency of $\phi_{OH}=1-\phi_H^{exp}/\phi_H^{max}=0.06$. Considering the experimentally uncertainties in the determination of $f_D(2)=0.42\pm0.05$ and $\phi_H^{exp}=1.7\pm0.2$ an upper limit for ϕ_{OH} is obtained, $\phi_{OH}\leqslant0.10$.

We did not observe any increase in the H atom signal with increasing delay time between photolysis and detection pulse. Thus, the decay of the highly vibrationally excited molecule should be faster than 20 ns, the time resolution in the experiment. This is not surprising, because vibrationally excited four atomic molecules should dissociate on the picosecond time scale.

In a 193 nm photodissociation study of cyclopentadiene and indene Bersohn *et al.*[32] observed a dissociation time of about 100 ns for the 17 atomic indene and a much faster—not resolvable—decay of the 11 atomic cyclopentadiene. The mean kinetic energy of the H fragment was found to be $\langle E_{trans}(H)\rangle=4270\ cm^{-1}$ for cyclopentadiene significantly less than the available energy. In case of indene with its 45 vibrational degrees of freedom a longer time is needed before sufficient energy is released in the dissociation coordinate than in the case of cyclopentadiene with its 27 vibrational degrees of freedom. Thus, the fragmentation of HNOH or H_2NO (6 vibrational degrees of freedom) should be even faster.

Which one of the two H atoms is ejected first (H–ONH_2 or HONH–H) is a matter of speculation. There are only some hints that the N–H bond breaks first. If the H atom bond to the oxygen is ejected first, then the excited complex H_2NO should easier decay into H_2 and NO than into H+HNO because significantly less energy is required (see Table I). Furthermore, one expects vibrationally excited OH if the H–O and O–N bonds are stretched, which is not observed in the experiment.

In conclusion, the main dissociation channel in the photofragmentation of hydroylamine at 193 nm leads to hydrogen atoms with a quantum yield of 1.7 where the H products are sequentially ejected. The other dissociation channel ($OH+NH_2$) should have a quantum efficiency of less than 0.10.

ACKNOWLEDGMENTS

We are very grateful to Professor Dr. E. A. Reinsch for the *ab initio* calculation and useful discussions. This research was supported by the Deutsche Forschungsgemeinschaft.

[1] S. Tsunekawa, J. Phys. Soc. Jpn. **33**, 167 (1972).
[2] K. Tamagake, Y. Hamada, J. Yamaguchi, A. Hirakawa, and T. Tsuboi, J. Mol. Spectrosc. **49**, 232 (1974).
[3] M. E. Coles, A. J. Merer, and R. F. Curl, J. Mol. Spectrosc. **103**, 300 (1984).
[4] E. Lombardi, G. Tarantini, L. Pirola, and P. Torsellini, J. Chem. Phys. **64**, 5229 (1976).
[5] Y. Hamada and M. Tsuboi, Chem. Phys. **94**, 65 (1985).
[6] X. Luo, P. R. Fleming, T. A. Seckel, and T. R. Rizzo, J. Chem. Phys. **93**, 9194 (1990).
[7] X. Luo and T. R. Rizzo (to be published).
[8] V. Staemmler, Acta Phys. Pol. A **74**, 331 (1988).
[9] R. N. Smith and P. A. Leighton, J. Am. Chem. Soc. **66**, 172 (1944).
[10] R. A. Back and J. Betts, Can. J. Chem. **43**, 2157 (1965).
[11] J. Betts and R. A. Back, Can. J. Chem. **43**, 2678 (1965).
[12] C. De W. Hurd and H. J. Brownstein, J. Am. Chem. Soc. **47**, 67 (1925).
[13] K.-H. Gericke, S. Klee, F. J. Comes, and R. N. Dixon, J. Chem. Phys. **85**, 4463 (1986).
[14] K.-H. Gericke, Phys. Rev. Lett. **60**, 561 (1988).
[15] K.-H. Gericke, F. Schmidt, and F. J. Comes (to be published).
[16] M. H. Alexander *et al.* J. Chem. Phys. **89**, 1749 (1988).
[17] The energetic order of the Λ doublets of the four lowest rotational states of the $^2\Pi_{1/2}$ system is reversed.
[18] K.-H. Gericke, T. Haas, M. Lock, R. Theinl, and F. J. Comes, J. Phys. Chem. **95**, 6104 (1991).
[19] K. Dressler and D. A. Ramsay, Philos. Trans R. Soc. A **251**, 553 (1959); J. W. C. Johns, D. A. Ramsay, and S. C. Ross, Can. J. Phys. **54**, 1804 (1976); H. Lew, *ibid.* **54**, 2028 (1976).
[20] Ch. Jungen and A. J. Merer, Mol. Phys. **40**, 1 (1980); Ch. Jungen, K-E. J. Hallin, and A. J. Merer, *ibid.* **40**, 25 (1980).
[21] Ch. Jungen, K-E. J. Hallin, and A. J. Merer, Mol. Phys. **40**, 65 (1980).
[22] K.-H. Gericke, M. Lock, and F. J. Comes, Chem. Phys. Lett. **186**, 427 (1991).
[23] $\sigma(H_2S, 193\ nm)=6.4\times10^{-18}\ cm^2$, L. C. Lee, X. Wang, and M. Suto, J. Chem. Phys. **86**, 4353 (1987); $\sigma(NH_2OH, 193\ nm)=3.4\times10^{-18}\ cm^2$, J. Betts and R. A. Back, Can. J. Chem. **43**, 2678 (1965).
[24] R. Schinke, *Photodissociation dynamics* (Cambridge University, Cambridge, 1993).
[25] E. A. Moore and W. G. Richards, Phys. Scr. **3**, 223 (1971).
[26] D. L. Baulch, R. A. Cox, R. F. Hampson Jr., J. A. Kerr, J. Troe, and R. T. Watson, J. Phys. Chem. Ref. Data **13**, 1259 (1984).
[27] K. P. Huber and G. Herzberg, *Molecular Spectra and Molecular Structure, IV. Constants of Diatomic Molecules* (van Nostrand Reinhold, New York, 1979); J. Masanet, A. Gilles, and C. Vermeil, J. Photochem. **3**, 417 (1974); B. Gelernt, S. V. Filseth, and T. Carrington, Chem. Phys. Lett. **36**, 238 (1975).
[28] Estimated from mean bond dissociation enthalpies.
[29] R. Vasudev, R. N. Zare, and R. N. Dixon, J. Chem. Phys. **80**, 4863 (1984).
[30] K.-H. Gericke, H. G. Gläser, C. Maul, and F. J. Comes, J. Chem. Phys. **92**, 6548 (1990).
[31] E. A. Reinsch (private communication).
[32] W. Yi, A. Chattopadhyay, and R. Bersohn, J. Chem. Phys. **94**, 5994 (1991).